SCIENCE CHINA
Technological Sciences

•Article•

February 2022 Vol.65 No.2: 432–439
https://doi.org/10.1007/s11431-020-1794-2

Formation control of quad-rotor UAV via PIO

BAI TingTing[1], WANG DaoBo[1*] & MASOOD Rana Javed[2]

[1] *College of Automation Engineering, Nanjing University of Aeronautics and Astronautics, Nanjing 211106, China;*
[2] *Department of Electrical Engineering, Usman Institute of Technology, Karachi 75850, Pakistan*

Received October 14, 2020; accepted February 22, 2021; published online November 12, 2021

In this article, the formation control of quad-rotor unmanned aerial vehicle (UAV) via pigeon inspired optimization (PIO) is designed. The nonlinear mathematical model of the quad-rotor UAV is used by applying algebraic graph theory and matrix analysis. A high order consistent formation control algorithm with fixed control topology is designed by using a position deviation matrix to describe its formation. To control the attitude of quad-rotor UAVs, it is difficult to obtain a set of optimal solutions, and hence a PIO based algorithm with variable weight hybridization is proposed. The algorithm is mainly composed of two parts. First, according to the distance between the particles in the iterative process, the inertia weight is dynamically changed, and the coefficient is adjusted to control the degree of influence on its inertia weight. Second, the overall scenario is designed by using MATLAB based simulations which show that the formation control of the quad-rotor UAV is achieved with the help of PIO.

pigeon inspired optimization, formation control, unmanned aerial vehicle and quad-rotor UAV

Citation: Bai T T, Wang D B, Masood R J. Formation control of quad-rotor UAV via PIO. Sci China Tech Sci, 2022, 65: 432–439, https://doi.org/10.1007/s11431-020-1794-2

1 Introduction

Unmanned aerial vehicle (UAV) is achieving interest in numerous areas such as rescue, surveillance, replacing men in hazards, and in that environment where humans cannot easily reach [1]. The capability of the UAV fleet is a regular extension of each UAV control issue. The multiple UAVs form a more effective system than a single UAV. The initial formation of flying is a precondition for the cooperation between UAVs [2]. The most important requirement of each UAV is its guidance and navigation system through which the path-planning is achieved. Mostly, objectives of path planning are used to optimize an attained function under dynamic and kinetic constraints rather than a trajectory to the target. The path planning problem of the UAV can be modeled as a non-linear optimization problem that aims to find the shortest path from the initial position to the designated position [3–5].

During the last few decades, mankind achieved much success in autonomous flying robot systems by considering and tracking the characteristics of flying birds [6]. The concept of these types of robots is taken from the natural behavior of birds. As far as practical, applied and theoretical research is concerned, pigeon behavior has received more attention due to its simplicity and accuracy. Therefore, to control multiple UAVs' formation, the pigeon coordination behavior is considered to resolve group operation issues of the UAVs [7,8].

In order to carry out the desired operation, various unmanned aerial vehicles coordinate with each other to perform a specific task. A group of UAVs take off from different origins and then grouped in one formation after taking some initial meetup or target point. At present, formation control of multiple UAVs is amongst the latest research topic in control engineering [9]. Although the demand for cooperative control structure ranked lower in comparison with

*Corresponding author (email: dbwangpe@nuaa.edu.cn)

other control systems, there is a mandatory requirement of a cooperative control structure in multiple UAVs' formation [10–12]. Every single UAV must have the ability of adaptive decision making, planning, and autonomous controlling. With the help of a cooperative perception and avoidance algorithm, UAVs can form stable flight control for a specific combination and group movement. Additionally, formation control also elaborates the use of agent to agent communication, collects the neighbor's information to update their status, and achieves a consistent state. Previously, many researchers are interested in the formation control of multiple quad-rotor UAVs. Currently, many researchers are trying to solve the problems related to formation control and some have achieved great success [13].

Many research results explained that quad-rotor UAV is considered as a second-order integrator dynamic system. Through this standardization strategy, the controlling of multiple UAVs takes place. Moreover, the adaptive control method is used for the formation of multiple UAVs with unconfined and confined control of thrust, altitude, and attitude control. The most important requirement of the UAV is guidance and navigation systems of which path-planning is the basic component. Mostly, the aim of path planning is not only to produce a trajectory to a target but to optimize an attained function under dynamic and kinetic constraints. The path planning problem of the UAV can be modeled as a nonlinear optimization problem that aims to find a path from the start position to a mark position [14–17].

The major innovations of this manuscript are as follows. (1) Pigeon inspired optimization (PIO) algorithm is used by applying algebraic graph theory and matrix analysis. (2) The high order consistent formation control algorithm with fixed control topology is adopted, and the formation is described by position deviation matrix. (3) A PIO based algorithm with variable weight hybridization is designed in this article.

This research paper is arranged as follows. Sect. 1 describes the introduction. Sect. 2 defines the mathematical model. Formation control of the quad-rotor UAV is discussed in Sect. 3. Improved PIO algorithm is presented in Sect. 4. Finally, analysis and simulation results are provided in Sect. 5.

2 Modeling

In this section, the quad-rotor UAV model is designed for successful formation. To get the desired formation or configuration of UAVs, individual UAV must be controlled at the desired position or location to attain the coordinated control. The position control of the quad-rotor depends upon the attitude and speed control in all directions. This part of the manuscript demonstrates a mathematical model of the quad-rotor UAV along with its Earth's coordinate system and fixed body frame. Whereas the Earth's coordinate system is defined as X-axis points in the ground plane, Y-axis is perpendicular to X-axis in the ground plane and Z-axis is also perpendicular to the ground plane. These three axes (X, Y, Z) create the rectangular coordinate system. The fixed body coordinate system is attained by assuming that the mass of the quad-rotor UAV is uniformly distributed and the origin of the fixed body frame in the center of mass [18,19]. The relationship among the ground coordinate system and fixed body coordinate system is stated in terms of the rotational matrix as follows:

$$\mathbf{R}(\varphi,\theta,\psi)=\begin{bmatrix}\cos\theta\cos\psi & \cos\psi\sin\theta\sin\varphi-\sin\psi\cos\theta & \cos\psi\sin\theta\cos\varphi+\sin\psi\sin\varphi\\ \cos\theta\sin\psi & \sin\psi\sin\theta\sin\varphi+\cos\psi\cos\varphi & \sin\psi\sin\theta\cos\varphi-\cos\psi\sin\varphi\\ -\sin\theta & \cos\theta\sin\varphi & \cos\theta\cos\varphi\end{bmatrix}, \tag{1}$$

$$T_i=C_{T_i}\delta_i,\ i=1,2,3,4, \tag{2}$$

where T_i denotes the thrust, C_{T_i} is the thrust of the aerodynamic coefficient and δ_i is the angular velocity of the system. C_{T_i} and δ_i are typically used for actuator's speed. In a fixed body frame, the vertical direction is formed by each actuator in Z direction. The term F_{B} denotes the force of the fixed body frame:

$$F_{\mathrm{B}}=\begin{bmatrix}0\\0\\0\\\sum_{i=1}^{4}T_i\end{bmatrix}. \tag{3}$$

The forces of the UAV which are acting on Earth's coordinate system can be stated as

$$F_{\mathrm{B}}=\begin{bmatrix}\sum_{i=1}^{4}T_i(\cos\psi\sin\theta\cos\varphi+\sin\psi\sin\varphi)\\ \sum_{i=1}^{4}T_i(\cos\psi\sin\theta\cos\varphi+\sin\psi\sin\varphi)\\ \sum_{i=1}^{4}T_i(\cos\theta\cos\varphi)\end{bmatrix}. \tag{4}$$

Moreover, the mass of the UAV "m" is influenced to gravity "mg" acting towards downward. By considering the air resistance during the flight, the relationship among the UAV velocity and air resistance acting on the frame coordinate system is stated as

$$D_E=\begin{bmatrix}D_x\\D_y\\D_z\end{bmatrix}=\begin{bmatrix}-\frac{1}{2}|V_x|V_xC_{dx}\\-\frac{1}{2}|V_y|V_yC_{dy}\\-\frac{1}{2}|V_z|V_zC_{dz}\end{bmatrix}. \tag{5}$$

In eq. (5), V_x, V_y, V_z are the velocities, and C_{dx}, C_{dy}, C_{dz} are the drag coefficient along X, Y, Z directions respectively.

$$\begin{aligned}&m_\varphi=l(T_2-T_4),\\&m_\theta=l(T_1-T_3),\\&m_\psi=d(\delta_2^{\,1}+\delta_3^{\,2}-\delta_2^{\,2}-\delta_4^{\,2}),\end{aligned} \tag{6}$$

where "l" is the length of each arm of UAV, the yaw moment "m_ψ" is produced by the difference of velocity of each actuator and the yaw moment coefficient is d. The direction of each motor axis changes, when the attitude of quad-rotor UAV changes respectively. At that time, each actuator will generate a falling moment m_{gi}:

$$m_{gi}=H_{gi}\times\Omega=I_r\dot{\delta}_i\times\Omega,\ i=1,2,3,4. \tag{7}$$

The eq. (7) defines the rotational speed of the rotor axis of UAV which is denoted by "Ω", the angular momentum of each rotor along the motor axis is denoted by H_{gi}, and the inertia matrix is $\mathbf{I}_r$. By considering that a UAV has a certain motion in which it does not change the direction of its actuator's axis when it rotates along the Z axis in the airframe. The angular velocity of the airframe rotation is equal to the angular momentum of the motor axis, which is denoted as $\Omega=[p,q,0]^{\mathrm{T}}$. The inertial matrix of the rotor is described as follows:

$$\mathbf{I}_r=\begin{bmatrix}I_{rx}&0&0\\0&I_{ry}&0\\0&0&I_{rz}\end{bmatrix}. \tag{8}$$

The gyroscopic moment m_{gi} and m_g is the total gyroscope torque of a single rotor of UAV that can be obtained as follows:

$$m_g=\begin{bmatrix}-I_{rz}q\\I_{rz}p\\0\end{bmatrix}\dot{\delta}_i,\ i=1,2,3,4, \tag{9}$$

$$m_g=\begin{bmatrix}-I_{rz}q\\I_{rz}p\\0\end{bmatrix}(\delta_1+\delta_3-\delta_2-\delta_4). \tag{10}$$

The inertial gyroscopic moment m_{gb} for the identical principle of UAV motion is

$$m_{gb}=\begin{bmatrix}(I_y-I_z)qr\\(I_z-I_x)pr\\(I_x-I_y)pq\end{bmatrix}. \tag{11}$$

According to Newton's second law of motion and momentum formula, the force and moment analysis of the quad-rotor UAV and the relationship between angular velocity and attitude angle under insignificant turbulence in ground coordinates system establish the following equation of motion:

$$\begin{cases}m\ddot{x}=(\sin\theta\cos\varphi\cos\psi+\sin\varphi\sin\psi)U_1,\\m\ddot{y}=(\sin\theta\cos\varphi\sin\psi-\sin\varphi\sin\psi)U_1,\\m\ddot{z}=\cos\varphi\cos\theta\,U_1-m_g,\\I_x\ddot{\varphi}=\dot{\theta}\dot{\psi}(I_y-I_z)-I_{rz}\dot{\theta}\delta+U_2,\\I_y\ddot{\theta}=\dot{\theta}\dot{\psi}(I_z-I_x)-I_{rz}\dot{\theta}\delta+U_3,\\I_z\ddot{\psi}=\dot{\varphi}\dot{\theta}(I_x-I_y)+U_4,\\U_1=\sum_{i=1}^{4}T_1,\\U_1=l(T_3-T_1),\\U_2=l(T_4-T_2),\\U_1=d(\delta_1^{\,2}+\delta_2^{\,2}-\delta_2^{\,2}-\delta_4^{\,2}),\\\delta=(\delta_1+\delta_3-\delta_2-\delta_4).\end{cases} \tag{12}$$

At the earth coordinate system, the position vector of the UAV is denoted by (x, y, z), and (u, v, w) are the velocity vectors of the UAV. It can be seen from the core system of the UAV that there is no coupling relationship between the vertical and virtual motion [20]. The $\ddot{x}$ and $\ddot{y}$ are the forward and backward accelerations along the horizontal direction, i.e., pitch θ and roll φ angle. $\ddot{z}$ is the ascending and descending motion in the vertical axis. The motion of quad-rotor UAV should be satisfied by the following equations:

$$\begin{aligned}&a_{\min}\le\ddot{x}_i\le a_{\max},\\&a_{\min}\le\ddot{y}_i\le a_{\max},\\&|\theta_i|\le\theta_{\max},\\&|\varphi_i|\le\varphi_{\max},\\&\lambda_{\min}\le\ddot{z}_i\le\lambda_{\max},\end{aligned} \tag{13}$$

where $a_{\min}, a_{\max}, \theta_{\max}, \varphi_{\max}, \lambda_{\min}$, and $\lambda_{\max}$ represent the minimum acceleration, maximum acceleration, maximum pitch angle, maximum roll angle, minimum descending rate, and maximum ascending rate of the UAV, respectively.

3 Quad-rotor UAV formation control

3.1 Preliminaries

In this research, the communication model of the UAV is defined by the algebraic graph theory. Once the model is described, it is important to evaluate it. For the analysis of the communication model of the UAV, matrix theory is used. The algebraic graph consists of different nodes and ends [21]. The algebraic graph mainly falls into two classes: (1) directed graph and (2) undirected graph. With the help of these graphs, the communication model among the individuals of the UAVs formation system is explained and represented by $G=(V, E, A)$, where $V=(v_1,v_2,\cdots,v_n)$ re-

presents the group of nodes and $E \leq V \times V$ represents the set of edges. The directed path is represented by $(v_i, v_j) \leq E$ in a directed graph. The directed path shows that the jth node can get the information about the ith node. v_i is named as a parent node and v_j is named as a child node. $A = [a_{ij}] \in R^{N \times N}$ is called adjacent matrix with loads. When $(v_i, v_j) \leq E$, a_{ij} for each side assigned loads where $a_{ij}>0$ or $a_{ij}=0$, in undirected graphs. For a directed graph, if there is any directed path from one node to all other nodes it is called graph G directed spanning trees where $D = \mathrm{Diag}\{D_{\mathrm{out}1}, D_{\mathrm{out}1}, \cdots, D_{\mathrm{out}n}\} \in R^{N \times N}$ where $D_{\mathrm{out}i} = \sum_{i=1}^{n} a_{ij}$. Laplace matrix is $\mathbf{L}=D-A$ in which $L=[l_{ij}]R^{N \times N}$ where l_{ij} is expressed as

$$l_{ij} = \begin{cases} -a_{ij}, & v_j \in N_j, \\ \sum_{j \in N_i} a_{ij}, & v_j = v_i, \\ 0, & \text{other}, \end{cases} \tag{14}$$

where N_i is a node and v_i are the child nodes of the $N_i=\{v_j \in V : (v_i, v_j) \in E, j \neq i\}$.

3.2 Designing the control algorithm of high order consistent formation

Consider that the n quad-rotor UAV formation system comprises of members. In this section, the main goal is to use a linear sub-system beneath the fixed directed topology G. The designed control algorithm makes the position vectors of the individual rotor $\mathbf{r} = [x \quad y \quad z]^{\mathrm{T}}$ and attitude vector $\boldsymbol{\eta}= [\phi \quad \theta \quad \varphi]^{\mathrm{T}}$. In actual flight formation, the position vector of the individual quad-rotor cannot reach a similar value because the centroid of each quad-rotor cannot be met. In this research paper, the position deviation matrix is used to explain the formation. Suppose that Δ_{ij} is the relative position deviation of ith and jth structure of quad-rotor [22]. The matrix is composed of a positional deviation matrix which is denoted by r. With the help of these matrices, different formations can be planned by using different position deviation matrices $\mathbf{r}$. A consistent formation control algorithm is planned by using a fourth-order linear subsystem. The distributed consistency formation control algorithm is chosen for the system. The selected algorithm is as follows:

$$U'_{3i} = -\gamma_1 x_i^{(1)} - \gamma_2 x_i^{(2)} - \gamma_3 x_i^{(3)} - \beta \Sigma_{j \in N_i} a_{ij}(x_i - x_j - \Delta_{ij}), \tag{15}$$

where $i = \{1, 2, \cdots, n\}$, γ_k is the absolute information feedback gain, β is the relative information feedback gain, N_i is the set of the neighbor of ith quad-rotor, a_{ij} is the load connection, Δ_{ij} is the distance deviation of ith and jth quad-rotor in the x direction.

Definition 1: Let $\mathbf{X}_i = [X_i^{(0)}, X_i^{(1)}, X_i^{(2)}, X_i^{(3)}]^{\mathrm{T}}$, $\Delta_x = [\Delta_x, 0, 0, 0]^{\mathrm{T}}$. The states of the individual rotor satisfy the following condition under the initial condition.

$$\lim_{t \to \infty} \left| x_i - x_j - \Delta_x \right| = 0.$$

The above definition can incrementally solve the problem of the system. By solving the aforementioned problem, the applicability of high order consistency formation control is verified. The dynamics of ith quad-rotor based on the algorithm (15) can be stated as

$$\dot{x}_i = Ax_i - \Sigma_{j \in N_i} a_{ij} B(x_i - x_j - \Delta_x), \tag{16}$$

where $A = \begin{bmatrix} \mathbf{0} & \mathbf{I}_3 \\ \mathbf{0} & -\boldsymbol{\gamma}^{\mathrm{T}} \end{bmatrix}$ and $B = \begin{bmatrix} \mathbf{0} & \mathbf{O}_3 \\ \beta & \mathbf{O}^{\mathrm{T}} \end{bmatrix}$, $\boldsymbol{\gamma} = [\gamma_1, \gamma_2, \gamma_3]^{\mathrm{T}}$, $\mathbf{0} = [0, 0, 0]^{\mathrm{T}}$, $\mathbf{I}_3$ and $\mathbf{O}_3$ are identity matrices and zero matrices, respectively. If $\mathbf{x} = \left[x_1^{\mathrm{T}}, x_2^{\mathrm{T}}, \cdots, x_n^{\mathrm{T}}\right]^{\mathrm{T}}$ is the position of the entire quad-rotor UAV, the dynamics of the closed-loop network can be stated as

$$\dot{x} = [I_n \otimes A - (\mathbf{L} - \mathbf{R}_x) \otimes B]x = \varnothing_x, \tag{17}$$

where $\mathbf{L}$ is the Laplace matrix and $\mathbf{R}_x$ is the position deviation matrix of quad-rotor UAV formation system in x direction.

Let $n_i = Sx_i$ where $\eta_i = [\eta_{(4i-3)}, \cdots, \eta_{(4i)}]$, $i = 1, 2, \cdots, n$, and the transformation matrix $\mathbf{S}$ is then expressed as

$$\begin{bmatrix} 1 & 0 & 0 & 0 \\ 1 & S_1 & 0 & 0 \\ 1 & \Sigma_{i=1}^{2} S_1 & S_1 S_2 & 0 \\ 1 & \Sigma_{i=1}^{3} S_1 & \Sigma_{i=1}^{2} \Sigma_{j=1}^{3} S_i S_j & \Pi_{i=1}^{3} S_i \end{bmatrix}, \tag{18}$$

where $S_i \in P$, $i = 1, 2, ..., P$ is the finite set of positive numbers. After model transformation, the state of the closed-loop network is $\eta = \left[\eta_1^{\mathrm{T}}, \eta_2^{\mathrm{T}}, \cdots, \eta_n^{\mathrm{T}}\right]$, and the whole network is written as

$$\dot{\eta} = [I_n \otimes E - (L - R_x) \otimes F]\eta = \Psi_n, \tag{19}$$

where $F = B\Pi_{i=1}^{4} S_i$,

$$E = SAS^{-1} = \begin{bmatrix} -\frac{1}{S_1} & \frac{1}{S_1} & 0 & 0 \\ 0 & -\frac{1}{S_2} & \frac{1}{S_2} & 0 \\ 0 & 0 & -\frac{1}{S_3} & \frac{1}{S_3} \\ E_{4,1} & E_{4,2} & E_{4,3} & E_{4,4} \end{bmatrix}. \tag{20}$$

From $ES=SA$, we get $\Sigma_{i=1}^{4} E_{4,i} = 0$, if $E_{4,4} < 0$, $E_{4,i} > 0$, $E_{4,1} > \beta_{\max 1 \leq i \leq n}(l_{ii}) \Pi_{i-1}^{3} S_i$.

The consistency examination of the high order system can be extended through the convergence outcome of the first-order consistency control algorithm. According to Definition 1, the UAV grouped system could accomplish consistency under a fixed topology only if there is a spanning tree in the

directed graph G. Moreover, according to the transformation association, $U_{3i}^{'}$ control quantity is transformed into the actual control input U_{3i}.

$$U_{3i}=I_y/g\begin{cases}-\gamma_1 x_i^{(1)}-\gamma_2 x_i^{(2)}-\gamma_3 x_i^{(3)},\\ -\beta\sum_{j\in N_i}a_{ij}(x_i-x_j-\Delta_{xij}).\end{cases}\tag{21}$$

Similarly, the actual control input U_{2i} can be obtained:

$$U_{2i}=-I_x/g\begin{cases}-\gamma_1 x_i^{(1)}-\gamma_2 x_i^{(2)}-\gamma_3 x_i^{(3)},\\ -\beta\sum_{j\in N_i}a_{ij}(y_i-y_j-\Delta_{yij}).\end{cases}\tag{22}$$

The distributed consistency control algorithm for the second-order feature is written as

$$U'_{1i}=-\gamma_1\dot{z}_i-\beta\sum_{j\in N_i}a_{ij}(z_i-z_j-\Delta_{zij}).\tag{23}$$

Then the actual control input U_{1i} is written as

$$U_{1i}=m/\cos\phi\cos\theta\begin{cases}g-\gamma_1\dot{z}_i,\\ \beta\sum_{j\in N_i}a_{ij}(z_i-z_j-\Delta_{zij}).\end{cases}\tag{24}$$

The subsystem (23) is selected and the actual control input U_{4i} is attained which is written as

$$U_{4i}=I_z\left\{-\gamma_1\dot{\varphi}_i-\beta\sum_{j\in N_i}a_{ij}(\varphi_i-\varphi_j)\right\}.\tag{25}$$

The quad-rotor UAV consistency control algorithm design is accomplished. The simulation results confirm the validity of the algorithm.

4 Improved pigeon inspired optimization

4.1 PIO

PIO is defined as a group intelligence optimization algorithm. All the particles from the PIO algorithm provide the preferred set of possible solutions to the problem, by interacting with other particles. Updating itself constantly according to the robust function and state information of the whole group, in order to find the optimal solution of the desired problem [23–25].

In the N-dimensional space, the particle group consisting of M particles $X_i=x_{i1},x_{i2},x_{i3},x_{i4},\cdots,x_{in}$ represents the ith position of a particle in the nth dimensional space. $V_i=(v_{i1},v_{i2},v_{i3},\cdots,v_{in})$ represents the ith particle speed of $P_i=(p_{g1},p_{g2},p_{g3},p_{g4},\cdots,p_{gn})$.

In PIO each particle group passes over its own chronological and population optimal values during the iteration as shown below eqs. (26) and (27).

$$V_{kd}^{k+1}=\omega V_{id}^{k}+c_1r_1(p_{id}^{k}-X_{id}^{k})+c_2r_2(p_{gd}^{k}-X_{id}^{k}),\tag{26}$$

$$X_{id}^{k+1}=X_{id}^{k}+V_{id}^{k+1}.\tag{27}$$

In eqs. (26) and (27) for the inertia weight: d=1, 2, 3, $\cdots$, n; $i=1,2,3,\cdots,n$; acceleration is denoted by c_1, c_2 and their value must be greater than zero. r_1, r_2 are distributed among random numbers. The number of current iterations is denoted by k.

In eq. (28), the inertial weight ω defines the velocity of the particle inherited from the previous ability. It presents the linearly decreasing inertia weights. The larger value of inertia weight is in favor of the whole local search whereas the smaller inertial weights contributing to the local search.

$$\omega(k)=\frac{\omega_{\max}-k(\omega_{\max}-\omega_{\min})}{T_{\max}},\tag{28}$$

where $T_{\max}$ is the maximum number of iterations, $\omega_{\max}$, $\omega_{\min}$ are the maximum and minimum inertia weight values.

Eqs. (26) and (28) show that the starting inertial weight value ω is linearly decreasing with a large initial value and strong global search capabilities. In sequence, with the need for such particles that have the ability to explore the requirements, there are still some problems. First, if the particle group looking for the advantage it will converge towards the global most advantage, but the initial inertial weight value ω becomes larger, which results in slowing down the convergence speed. Second, because of late iteration, inertial weight value is gradually reduced, which in turn reduces the global search. It causes lack of diversity in particle group, and it is easy to fall in the local optimal.

L_{ki} represents the kth iteration of the i particles and the current most distance of the optimal particle, $L_{ki\max}$ represents the maximum particles of i and k iterations, and $L_{ki\min}$ represents the minimum particles of i and k iterations.

The following equation shows the relationship between the weight of the particle inertia and the size of the distance.

$$\omega_d=\omega_{\min}+\frac{(L_{ki}-L_{ki\min})(\omega_{\max}-\omega_{\min})}{L_{ki\max}-L_{ki\min}}.\tag{29}$$

The following equation shows the weight of the particle inertia at the kth iteration:

$$\omega_k=\omega_{\max}-\frac{k(\omega_{\max}-\omega_{\min})}{T_{\max}},\tag{30}$$

where $T_{\max}$ is the maximum number of iterations and $\omega_{\max}$, $\omega_{\min}$ are the maximum and minimum inertia weight values. Combining the above two equations, inertial weights can be obtained by the following formula:

$$\begin{cases}\omega=a\omega_d+b\omega_z,\\ a+b=1,\end{cases}\tag{31}$$

where a, b are constants.

4.2 Improved strategies for inertia weights

The number of iterations increases in the process due to the introduction of inertial weights, which results in stronger optimal particles control so that the whole particle gradually decreased. Hybridization h is defined as a continuous iterative process. The particle group is most likely to fall into the

local optimality if the global optimum has not changed. The hybridization process is defined as

$$P_{\text{new}}(x_i) = cP_{\text{select}}(x_i) + (1-c)P_{\text{current}}(x_i). \tag{32}$$

In eq. (32), P_{new} represents the newly generated particles, P_{select} represents the selection of superior particles, P_{current} represents contemporary new generation particles, and c is a random variable between [0,1].

4.3 Improving group optimization

(1) Set the velocity and position of all elements as per the fitness function value criteria in order to select the maximum history and optimal particles.

(2) Calculate the distance between the individual particles and the current global optimal position; get $L_{ki\max}$, $L_{ki\min}$ by eq. (29) and update the inertia weight of each particle in the next iteration ω.

(3) Determine the distance of individual particle and current global optimization and update the inertia weight of all particles in the next iteration from eq. (29) $L_{ki\max}$, $L_{ki\min}$.

(4) According to eqs. (26)–(31) update the position and velocity of each particle and calculate the appropriate degree of value.

(5) If the current fitness value of the particles is greater than its historical value, then it is considered a good value.

(6) It is determined whether the hybridization conditions are satisfied, i.e., a continuous generation of h global optimal value remains unchanged.

(7) Select the Q optimum particle root from M particles according to the eq. (32) hybridization to produce new particles which replace the old particles, and start from step (2) again.

(8) To determine whether the termination condition is satisfied, the output is global optimum; otherwise, go to step (3).

5 Simulation and results

5.1 Settings of simulation parameters

Small quad-rotor UAVs fly in the formation from their initial position to achieve a uniform combination. The parameters of each quad-rotor UAV are as follows: M=2.5 kg; I_{xx}= 0.011 kg/m^2; I_{yy}=0.011 kg/m^2; I_{zz}=0.035 kg/m^2; g=9.8.

The position vectors of each quad-rotor UAV at the initial positions are as follows:

$$X = [100 \quad 67 \quad 82 \quad 52]^{\text{T}}, \tag{33}$$

$$Y = [100 \quad 55 \quad 88 \quad 72]^{\text{T}}, \tag{34}$$

$$Z = [90 \quad 60 \quad 100 \quad 75]^{\text{T}}. \tag{35}$$

The attitude vectors at the initial position are zero. For simplicity, the weights of the network are assumed as 0 or 1. The value is assumed 1 when there is a communication between two UAVs; otherwise it is assumed as 0. The communication topology of quad-rotor UAVs is given below (Figure 1).

The two flight formation processes are as follows.

(1) In the initial stage, an individual quad-rotor UAV hovers at a free position. Ultimately, they reach the same altitude at x and y.

(2) Each quad-rotor is hovering at a free position. Finally, they reach a position with an altitude difference at x and y, and thus form a formation in square shape.

The position deviation matrices are as follows:

$$R_x = \begin{bmatrix} 0 & -10 & -10 & 0 \\ 10 & 0 & 0 & 10 \\ 10 & 0 & 0 & 10 \\ 0 & -10 & -10 & 0 \end{bmatrix}, \tag{36}$$

$$R_y = \begin{bmatrix} 0 & 0 & 10 & -10 \\ 0 & 0 & 10 & 10 \\ -10 & -10 & 0 & 0 \\ -10 & -10 & 0 & 0 \end{bmatrix}, \tag{37}$$

$$R_{z1} = 0_4, \tag{38}$$

$$R_{z2} = \begin{bmatrix} 0 & 0 & 10 & -10 \\ 0 & 0 & 10 & 10 \\ -10 & -10 & 0 & 0 \\ -10 & -10 & 0 & 0 \end{bmatrix}. \tag{39}$$

5.2 Results and analysis

Figures 2 and 3 show that each quad-rotor is in different positions and directions. It is also noticed that the position of each quad-rotor changes gradually. Around X and Y, uniform aggregation is achieved after 18 s and each of them maintains the relative position difference. Around Z, the uniform aggregation is achieved after 8 s and similarly, each of them maintains relative position difference as in X and Y direction.

Figure 4 shows that each quad-rotor finally gathers the formation from various initial positions. They all keep the stable formation and the consistency control algorithm is effective.

Figure 5 shows that the quad-rotors are in the hovering stage at the initial condition and attitude angles are zero. As

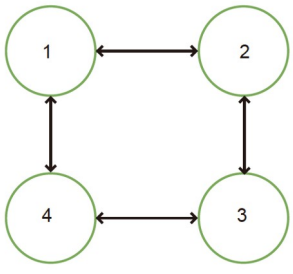

Figure 1 Simulation topology.

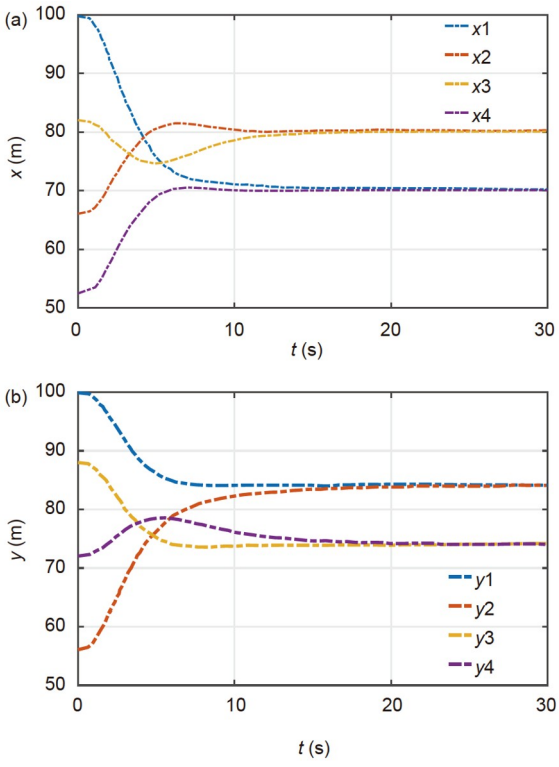

Figure 2 Formation of quad-rotors in X and Y directions.

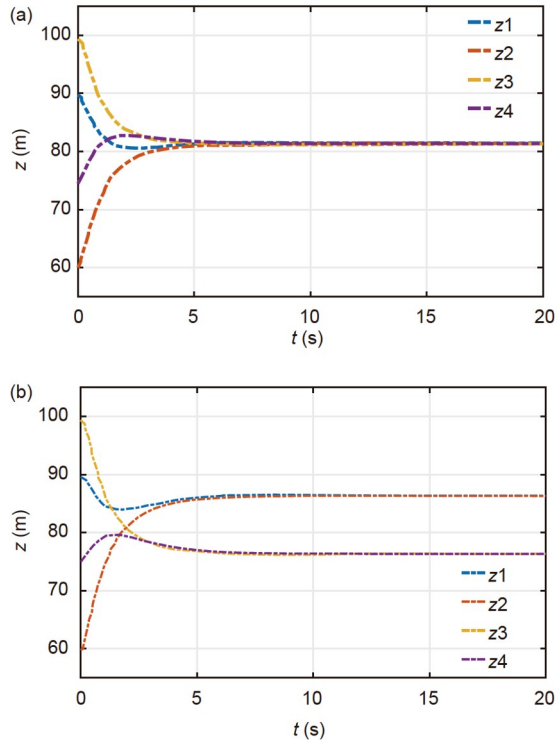

Figure 3 Formation of quad-rotors in Z direction.

the position changes, the attitude angles gradually change and then finally stabilize to zero. Due to the similarity of

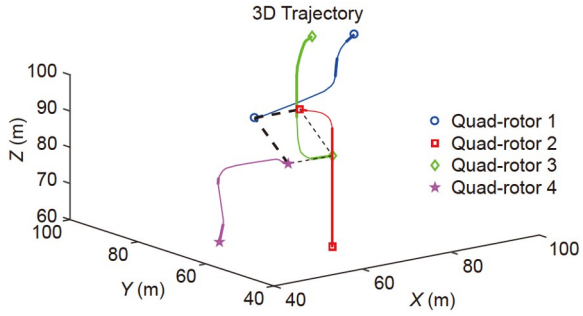

Figure 4 3D train of flight formation.

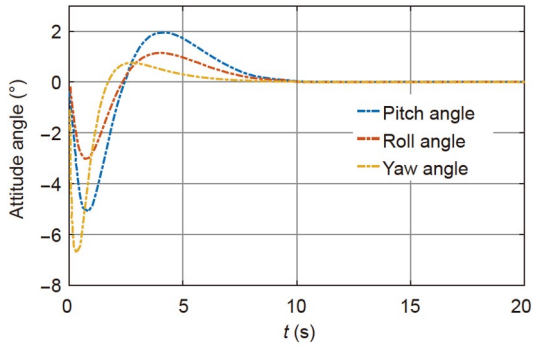

Figure 5 Change process of attitude angle of quad-rotor 1.

attitude angles of other quad-rotors, others will follow the same behaviour.

6 Conclusion

In this article, the mathematical model of quad-rotor UAV is utilized to make a set of four rotor-craft subsystems using algebraic graph theory and matrices analysis with the help of PIO. Moreover, a high-order consistent formation control algorithm with fixed control topology is adopted, and its formation is described by position deviation matrix. The simulated results show that the designed control algorithm runs successfully along with better transient and steady-state errors.

1 Mohamed N, Al-Jaroodi J, Jawhar I, et al. Unmanned aerial vehicles applications in future smart cities. Tech Forecast Soc Change, 2020, 153: 119293
2 Ronchi, Alfredo M. Safety and Security. In: e-Citizens. Cham: Springer, 2019. 43–108
3 Sharif Azadeh S, Bierlaire M, Maknoon M Y. A two-stage route optimization algorithm for light aircraft transport systems. Transp Res Part C Emerg Technol, 2019, 100: 259–273
4 Coutinho W P, Battarra M, Fliege J. The unmanned aerial vehicle routing and trajectory optimisation problem, a taxonomic review. Comput Ind Eng, 2018, 120: 116–128
5 Patley A, Bhatt A, Maity A, et al. Modified particle swarm optimization based path planning for multi-UAV formation. AIAA Parper, 2019. AIAA 2019-1167
6 Cliff O M, Saunders D L, Fitch R. Robotic ecology: Tracking small

dynamic animals with an autonomous aerial vehicle. Sci Robot, 2018, 3: eaat8409
7 Qiu H, Duan H. A multi-objective pigeon-inspired optimization approach to UAV distributed flocking among obstacles. Inf Sci, 2020, 509: 515–529
8 Xing D, Zhen Z, Gong H. Offense-defense confrontation decision making for dynamic UAV swarm versus UAV swarm. Proc Inst Mech Eng Part G, 2019, 233: 5689–5702
9 Janebäck E, Matilda K. Friendly robot delivery: Designing an autonomous delivery droid for collaborative consumption. Dissertation for Master's Degree. Göteborg: Chalmers University of Technology, 2019
10 Pang S, Wang J, Liu J, et al. Three-dimensional leader-follower formation control of multiple autonomous underwater vehicles based on line-of-sight measurements using the backstepping method. Proc Inst Mech Eng Part I, 2018, 232: 819–829
11 Pantelimon G, Tepe K, Carriveau R, et al. Survey of multi-agent communication strategies for information exchange and mission control of drone deployments. J Intell Robot Syst, 2019, 95: 779–788
12 Ma Y, Zhao Y, Qi X, et al. Cooperative communication framework design for the unmanned aerial vehicles-unmanned surface vehicles formation. Adv Mech Eng, 2018, 10: 168781401877366
13 Ayaz M. Comparative study of indoor navigation systems for autonomous flight. TELKOMNIKA, 2018, 16: 118–128
14 Baca T, Hert D, Loianno G, et al. Model predictive trajectory tracking and collision avoidance for reliable outdoor deployment of unmanned aerial vehicles. In: Proceedings of the 2018 IEEE/RSJ International Conference on Intelligent Robots and Systems (IROS). New York: IEEE, 2018. 6753–6760
15 Bhatt A, Maity A, Das K. Path planning for UAV using Sniff-Dog-Algorithm. In: The Proceedings of 2018 International Conference on Unmanned Aircraft Systems (ICUAS). New York: IEEE, 2018. 692–701
16 Navaneethkrishnan B, Pranjal B, Saumya K S, et al. State-space identification of unmanned helicopter dynamics using invasive weed optimization algorithm on flight data. arXiv: 1809.05021
17 Oruc B E, Kara B Y. Post-disaster assessment routing problem. Transp Res Part B, 2018, 116: 76–102
18 de Angelis E L, Giulietti F, Rossetti G. Multirotor aircraft formation flight control with collision avoidance capability. Aerosp Sci Tech, 2018, 77: 733–741
19 Bonyan Khamseh H, Janabi-Sharifi F, Abdessameud A. Aerial manipulation—A literature survey. Robot Auton Syst, 2018, 107: 221–235
20 Bernard M, Kondak K, Maza I, et al. Autonomous transportation and deployment with aerial robots for search and rescue missions. J Field Robot, 2011, 28: 914–931
21 Han T, Guan Z H, Wu Y, et al. Three-dimensional containment control for multiple unmanned aerial vehicles. J Franklin Inst, 2016, 353: 2929–2942
22 Sovinec C R, Glasser A H, Gianakon T A, et al. Nonlinear magnetohydrodynamics simulation using high-order finite elements. J Comput Phys, 2004, 195: 355–386
23 Duan H, Qiao P. Pigeon-inspired optimization: A new swarm intelligence optimizer for air robot path planning. Int J Intell Comput Cybernet, 2014, 7: 24–37
24 Duan H, Luo Q. New progresses in swarm intelligence-based computation. Int J Bio Inspir Comput, 2015, 7: 26
25 Zhang S, Duan H. Gaussian pigeon-inspired optimization approach to orbital spacecraft formation reconfiguration. Chin J Aeronaut, 2015, 28: 200–205